HHS Public Access

Author manuscript

Nat Nanotechnol. Author manuscript; available in PMC 2019 April 08.

Published in final edited form as:

Nat Nanotechnol. 2018 December ; 13(12): 1174–1181. doi:10.1038/s41565-018-0271-3.

A Malaria Vaccine Adjuvant Based on Recombinant Antigen Binding to Liposomes

Wei-Chiao Huang[1], **Bingbing Deng**[2], **Cuiyan Lin**[1], **Kevin A. Carter**[1], **Jumin Geng**[1], **Aida Razi**[3], **Xuedan He**[1], **Upendra Chitgupi**[1], **Jasmin Federizon**[1], **Boyang Sun**[1], **Carole A. Long**[2], **Joaquin Ortega**[3], **Sheetij Dutta**[4], **C. Richter King**[5], **Kazutoyo Miura**[2], **Shwu-Maan Lee**[5], and **Jonathan F. Lovell**[1,*]

[1]Department of Biomedical Engineering, University at Buffalo, State University of New York, Buffalo, New York 14260, USA

[2]Laboratory of Malaria and Vector Research, National Institute of Allergy and Infectious Diseases, National Institutes of Health, Rockville, Maryland 20852, USA

[3]Department of Anatomy and Cell Biology, McGill University Montreal, Quebec, H3A 0C7, Canada

[4]Walter Reed Army Institute of Research, Silver Spring, Maryland 20910, USA

[5]PATH's Malaria Vaccine Initiative (MVI), Washington, DC 20001, USA

Abstract

Pfs25 is a malaria transmission-blocking vaccine antigen candidate, but its apparently limited immunogenicity in humans has hindered clinical development. Here, we show that recombinant, his-tagged Pfs25 can be mixed at the time of immunization with pre-formed liposomes containing cobalt-porphyrin-phospholipid (CoPoP), resulting in spontaneous nanoliposome antigen particleization (SNAP). Antigens are stably presented in uniformly-oriented display via his-tag insertion in the CoPoP bilayer, without covalent modification or disruption of antigen conformation. SNAP immunization of mice and rabbits is well tolerated with minimal local reactogenicity and results in orders-of-magnitude higher functional antibody generation compared to other "mix-and-inject" adjuvants. Serum-stable antigen-binding during transit to draining lymph nodes leads to enhanced antigen uptake by phagocytic antigen presenting cells, with subsequent generation of long-lived, antigen-specific plasma cells. Seamless multiplexing with four additional

* jflovell@buffalo.edu.

Contributions

W.C.H., C.R.K, S.M.L. and J.F.L conceived the project. W.C. H., K.M, S.M.L. and J.F.L designed most experiments. W.C.H. and J.F.L wrote the manuscript. W.C.H., C.L., and J.G. performed animal experiments. W.C.H., C.L., B.D., C.A.L. and K.M. performed and interpreted ELISA and SMFA experiments. A.R. and J.O. performed Cryo-TEM. W.C.H., K.C., C.L., X.H. and B.S. produced and characterized liposomes. X.H. performed splenocyte studies. U.C and W.C.H. produced fluorescently-labeled antigens. J.F. performed circular dichroisim studies. S.D and S.M.L. produced antigens.

Ethics statement

All mice experiments were carried out using protocols approved by the University at Buffalo Institutional Animal Care and Use Committee (IACUC). All rabbit experiments were carried out using protocols approved by the Pocono Rabbit Farm IACUC.

Data availability

All raw data are available upon request.

his-tagged *Plasmodium falciparum* polypeptides induces strong and balanced antibody production, illustrating the simplicity of developing multi-stage particulate vaccines with SNAP immunization.

An effective malaria vaccine would be instrumental in eliminating the disease, which causes over 200 million cases and nearly half a million deaths annually.[1] One unique approach is a transmission-blocking vaccine (TBV). TBVs cause immunized hosts to transfer induced antibodies to mosquitos during a blood meal, blocking parasite development in the mosquito gut. A vaccine that reduces parasite transmission is part of the World Health Organization Malaria Vaccine Technology roadmap, but has not yet been evaluated in large-scale trials due in part to challenges in developing a TBV that produces high and sustained transmission-blocking antibodies.[2, 3]

P. falciparum Pfs25 is an intensively-studied TBV antigen candidate.[4–6] The 25 kDa protein contains 11 disulfide bonds, so production of properly folded Pfs25 is of interest.[7–10] Clinical trials with Pfs25 or *P. vivax* Pvs25 failed to produce satisfactory levels of antibodies using Alum as a vaccine adjuvant, and use of Montanide ISA-51 as an adjuvant resulted in unexpected local reactogenicity.[11, 12] The limited immunogenicity of Pfs25 may be related to its compact structure and putative hapten-like behavior.[13]

Antigen-engineering has been pursued to improve induction of antibodies against Pfs25. This includes conjugation to protein toxins (from Pseudomonas[14], cholera[15, 16], or tetanus[13]); conjugation to nanoparticles (such as gold[17] or polymer[18]); engineering Pfs25 in virus-like particles (VLPs)[19]; and use of viral vectors[20]. Emerging approaches include the use of recombinant protein tags for downstream Pfs25 multimerization [21] or attachment to VLPs[22]. While these strategies hold potential, genetically-engineered constructs or conjugation strategies are time and resource consuming, can induce heterogeneous antigen populations, can mask important epitopes, risk incorrect folding, and can impede target antigen characterization within the resulting constructs.

Liposomes containing cobalt-porphyrin-phospholipid (CoPoP) can be stably functionalized by simple mixing with proteins bearing a polyhistidine-tag (his-tag); a small 6–10 stretch of histidine residues that is used in recombinant protein purification.[23] A C-terminus his-tagged and glycosylation-free Pfs25 was recently produced in a baculovirus system.[10] The 11 disulfide bonds of this protein match the predicted structure of the analogous *P. vivax* Pvs25.[24] Here, we make use of this well-characterized his-tagged antigen for spontaneous nanoliposome antigen particleization (SNAP). Spontaneous particleization (i.e., binding of soluble, recombinant antigens to nanoliposomes so that they decorate the surface of the colloidal particles) occurs when the antigens stably bind to membranes via insertion and coordination of the his-tag into bilayers containing CoPoP.

Spontaneous nanoliposome antigen particleization (SNAP)

We formed liposomes with two active lipids; synthetic monophosphoryl lipid A (PHAD), a toll-like receptor 4 agonist; and CoPoP, which is biologically inert but confers spontaneous his-tag antigen particelization. Two passive lipids completed the formulation; dipalmitoyl phosphatidylcholine (DPPC) and cholesterol (CHOL). Liposomes were produced with a

mass ratio of [4:2:1:1] of [DPPC:CHOL:CoPoP:PHAD] unless otherwise indicated. Native polyacrylamide gel electrophoresis showed that with simple mixing, Pfs25 bound to liposomes containing CoPoP, but not to liposomes containing porphyrin-phospholipid (PoP), which are identical but lack cobalt (Fig 1a). Liposomes containing a nickel-chelating headgroup lipid (Ni-NTA) did not stably bind Pfs25. With CoPoP, the his-tag buries itself within the hydrophobic cobalt-porphyrin bilayer and coordinates with the metal, resulting in attachment that is stable in biological media. Liposomal Ni-NTA approaches for binding his-tagged ligands are unstable in biological media.[25–27] Liposomal Co-NTA has been explored for immunization, although the approach was found to be inferior to covalent linkage.[28] We previously found that Co-NTA cannot stably bind his-tagged peptides.[27]

When varying amounts of CoPoP/PHAD liposomes were incubated with Pfs25, a 4:1 mass ratio of PHAD to protein was sufficient for binding (Fig 1b). This is equivalent to a CoPoP-to-Pfs25 mass ratio of 4:1, and a lipid-to-Pfs25 mass ratio of 320:1. Pfs25 did not bind PoP/PHAD liposomes. A similar trend was observed with a microcentrifugal filtration binding assay (Fig 1c-d). Lysozyme, a protein without a his-tag, did not bind to CoPoP liposomes (Fig 1d). Approximately 80 % Pfs25 binding was achieved at room temperature in 3 hrs (Fig 1e). These particleization conditions (4:1 mass ratio of CoPoP (320 μg/mL) to Pfs25 (80 μg/mL)), incubated without shaking at room temperature for 3 hrs) were fixed for all studies, and the desired dosing was achieved by subsequent dilution in buffered saline.

His-tagged Pfs25 exhibited a low alpha helical content based on circular dichroisim, consistent with the structure of the same protein in an antibody complex (Fig S1).[29] Following Pfs25 binding to CoPoP liposomes, we assessed whether monoclonal antibodies (mAbs) recognized the correctly-folded protein conformation. 4B7 has been reported to be a conformational specific mAb.[4] Recently, two non-overlapping epitopes have been identified by functional mAbs (1269 and 1245).[29] The 1269 mAb binds to a similar epitope as 4B7, while 1245 binds a distinct region. Following incubation with Pfs25-specific mAbs, protein G beads were used to immunoprecipitate the entire liposome-antigen complex, which was then detected by endogenous PoP or CoPoP fluorescence following detergent disruption. As shown in Fig 1f, 4B7, 1269 and 1245 immunoprecipitated whole CoPoP liposomes bound with his-tagged Pfs25, but not PoP liposomes (which do not bind Pfs25). As both 1269 and 1245 bind to Pfs25 in a reduction sensitive fashion, these results suggest that particleized Pfs25 maintains a correct conformation. A mAb against a HIV envelope segment (2F5) and another TBV antigen, Pfs48/45 (3E12), served as negative controls.

Cryo-electron microscopy revealed that CoPoP/PHAD liposomes were small and unilamellar, with a spherical size close to 100 nm (Fig 1g). Following Pfs25 binding, liposome curvature changed subtly, into more oblong structures (Fig 1h). Individual proteins were not visible, due to their small size. Based on light scattering, the liposomes were approximately 100 nm in diameter (Fig S2a). Minimal change in size or polydispersity was induced by SNAP (Fig S2a, S2b). SNAP did not substantially impact CoPoP/PHAD liposome surface charge (Fig S2c) which was had a negative zeta potential, consistent with other observations of liposomes containing MPLA.[30]

Refrigerated storage stability was assessed over a 9-month period. Minimal change was observed in liposome size, which was close to 100 nm (Fig S3a) or polydispersity index, which remained less than 0.1 (Fig S3b). Spontaneous Pfs25 binding capacity of the liposomes remained intact throughout (Fig S3c). Four separate batches of CoPoP/PHAD liposomes exhibited similar size, polydispersity and capacity for Pfs25 binding (Fig S3d-f).

Antigen particleization induces strong antibody responses

Mice were immunized intramuscularly with 100 ng of Pfs25, mixed just prior to vaccination with Alum, Montanide ISA720, CoPoP liposomes, or CoPoP/PHAD-3D6A (3D6A) liposomes. 3D6A is a structurally similar form of PHAD used in our initial immunization studies. In all immunizations, a fixed mass ratio for [PHAD: Pfs25] of [4:1] was used. No additional purification steps were taken after combining the antigen with the adjuvants. As shown in Fig 2a, all CoPoP liposome induced production of IgG that was functional in a standard membrane feeding assay (SMFA). Liposomes lacking cobalt produced orders of magnitude lower anti-Pfs25 IgG and did not induce SMFA activity (Table S1). At 100 and 30 ng dosing, both CoPoP/PHAD liposomes and CoPoP liposomes induced strong IgG and full SMFA activity (Fig 2b, Table S2). However, at a 10 ng dose of Pfs25, only CoPoP/PHAD liposomes induced antibody production with full SMFA activity. At 100 ng Pfs25, inclusion of PHAD resulted in higher production of IgG2a and a higher IgG2a to IgG1 ratio, compared to CoPoP liposomes lacking PHAD (Fig S4a,b).

Further dose de-escalation was performed in mice. CoPoP/PHAD liposomes that included the saponin QS21 were also examined. With this DPPC-based formulation, QS21 induced liposome aggregation, although Pfs25 binding was not impaired (Fig S5). Addition of QS21 did not enhance Pfs25 antibody production (Fig 2c) and appeared to decrease IgG2a production (Fig S4c, d). CoPoP/PHAD liposomes induced antibodies that were effective in the SMFA at antigen doses down to 4 ng (Table S3). This corresponds to 16 ng of PHAD, which is a thousand fold lower than what is typically used for murine immunization.[30]

Safety studies were carried out using high doses of CoPoP. To ascertain whether CoPoP itself is tolerated, we formed CoPoP liposomes with 95 molar % CoPoP, along with 5 % polyethylene glycol distearoylphosphoethanolamine (PEG-lipid) for colloidal stability. CoPoP liposomes were then directly injected intravenously in mice at a dose of 100 mg/kg (CoPoP). This CoPoP dose is approximately 138,000 times higher than the minimum dose administered to mice that induced functional SMFA activity (4 ng Pfs25 and 16 ng CoPoP). Another group of mice was injected intramuscularly with a single dose of 20 μg Pfs25 adjuvanted with CoPoP/PHAD liposomes, corresponding to a 5000-fold higher dose than the minimum functional dose. Mice exhibited normal weight gain (Fig 2d). A complete blood cell count (Fig S6a) and serum chemistry panel analysis (Fig S6b) two weeks following treatment revealed no statistically significant differences compared to healthy mice. No obvious differences in the liver, lungs, kidney or spleen of mice were observed with histology (Fig S6c). Thus, CoPoP liposomes appear to be well tolerated, although additional toxicity studies are required. Vitamin B12, a cobalt (III) porphyrin-related macrocycle, has been administered intravenously to healthy human volunteers at 5 gram dosing[31], and with repetitive milligram intramuscular dosing[32].

To assess whether SNAP immunization elicits transmission blocking antibodies in rabbits, intramuscular immunization was carried out with 10 μg of Pfs25 on day 0 and 28. When mixed with CoPoP/PHAD liposomes, but not Alum, strong anti-Pfs25 IgG titers were induced by day 56, and also pre-boost on day 28 (Fig 2e). The post-immune sera from the rabbits immunized with SNAP, but not Alum, produced transmission blocking activity in the SMFA (Fig 2f, Table S5). Even at a 10-fold lower antigen dose, of 1 μg Pfs25 (4 μg PHAD), transmission blocking antibody activity was induced in 2 of 3 rabbits immunized with SNAP.

Vaccine mechanism

We next sought to elucidate mechanistic insights into SNAP immunization, which is hypothesized to operate at multiple steps of immune activation (Fig 3a). Serum-stable antigen particleization enables the intact transit of the antigen-liposome complexes to draining lymph nodes, where they are more avidly uptaken by immune cells. Additional factors including recruitment of immune cells to the draining lymph nodes and downstream activation of dendritic cells likely contribute in the formation of germinal centers, recruitment of T-folicular helper (Tfh) cells and ultimately the generation of long-lived, antigen-specific plasma cells.

To monitor antigen-adjuvant association, Pfs25 was labeled with a fluorescent dye, Oyster-488, to generate Pfs25–488. When Pfs25–488 was incubated with CoPoP/PHAD liposomes, but not PoP/PHAD liposomes, fluorophore proximity to the CoPoP chromophore induced fluorescence quenching. When incubated in human serum for 2 weeks at 37 °C, Pf25–488 binding to CoPoP/PHAD liposomes remained intact, whereas no binding occurred with PoP/PHAD liposomes (Fig 3b). Following the 2-week incubation period, fluorescence of the dye could be restored upon dissociation (Fig S7a, b). Binding was also stable in bovine serum (Fig S7c).

To investigate the innate response, 100 ng Pfs25 was mixed with CoPoP/PHAD liposomes or Alum and intramuscularly administered to mice. Immune cell recruitment in draining lymph nodes was measured 48 hours following injection using a flow cytometry discrimination approach (Fig S8a).[33, 34] CoPoP/PHAD liposomes induced higher recruitment of macrophage and infiltrating monocytes compared to Alum (Fig 3c). An increased level of $CD11b^{-}$DCs was noted both Alum and CoPOP/PHAD liposomes groups. $Cd11b^{-}$DC cells play a role in cellular adaptive immune responses[35–37] In immunized mice, splenocytes produced interferon gamma when incubated with the antigen, demonstrating the involvement of T-cells (Fig S9). Other immune cell types (eosinophils, neutrophils, $CD11b^{low}$ DCs and myeloid DCs) did not increase in draining lymph nodes. The increased levels of certain immune cells in draining lymph nodes, by 2–3 fold, does not fully account for the drastic enhancement in antibody production induced by SNAP.

Following injection of fluorescently-labeled Pfs25–488, lymphatic antigen drainage was modulated relative to Alum, resulting in greater lymph node accumulation which may have some positive impact on immunogenicity (Fig S10). However, the enhanced lymph node

biodistribution of just several folds could also not account for the greater antibody response by several orders of magnitude.

The uptake of the antigen-liposome complex into antigen presenting cells (APCs) was next examined *in vitro* with fluorescence microscopy (Fig 3d). When Pfs25–488 was incubated with RAW264.7 murine macrophages, no cellular antigen uptake was observed. No antigen uptake was observed when Pfs25–488 was mixed with PoP/PHAD liposomes. However, the fluorescence of the liposomes themselves was detected, since macrophages avidly uptake liposomes.[38, 39] When Pfs25 was presented on liposomes using SNAP with CoPoP/PHAD liposomes, both antigen and liposome uptake occurred. Quantitative measurement of Pfs25 uptake confirmed this trend in both murine macrophages and murine bone marrow-derived DCs (BMDCs), another class of APC (Fig 3e). In the presence of cytochalasin B, a phagocytosis inhibitor, diminished Pfs25 uptake occurred, suggesting that a phagocytic uptake mechanism.

We next examined whether enhanced uptake of Pfs25 in APCs occurred in draining lymph nodes. As shown in Fig 3f and Fig S11, 2 days following SNAP immunization of mice, Pfs25 was uptaken in all major types of antigen presenting cells (APCs), including B-cells (B220), macrophages (F4/80), dendritic cells (CD11c) and MHCII-expressing cells (I-A/I-E). In contrast, when adjuvanted with alum, ISA720 or non-particleizing PoP/PHAD liposomes, there was minimal Pfs25 uptake into the most APC-types. Thus, improved delivery to APCs appears to be a key mechanism in which SNAP exerts enhanced immunogenicity compared to other adjuvants.

Maturation of DCs involves up-regulation of surface receptors, including CD40 and CD80. When BMDCs were incubated with Pfs25 for 24 hr increased CD40 and CD80 production when the antigen was comboined with CoPoP/PHAD liposomes, compared to the protein alone or with liposomes lacking PHAD (Fig 3g, Fig S12). PHAD has been shown to stimulate BMDC activation.[40] Thus, concomitant DC activation by PHAD may provide an additional mechanism of enhanced immune response.

Germinal center (GC) cell formation and recruitment of T follicular helper (Tfh) cells were assessed. GC B cells were identified by gating on $B220^+$ cells, and examining $CD95^+GL7^+$ cells (Fig S13), Tfh cells were gated on $CD4^+$, then identified with $PD1^+CXCR5^+$ staining (Fig S14). A week following murine intramuscular immunization, when combined with CoPoP/PHAD liposomes, Pfs25 induced a higher number of GC B cells and Tfh cells in draining lymph nodes (Fig 3h, i). There was no increase in these cell populations when Pfs25 was administered with Alum.

Efficacy of SNAP immunization

The durability of the antibody response for a TBV is important. A recent study using Pfs25-toxin conjugates reported antibody half-lives in the 50–100 day range.[13] Following SNAP immunization with 100 ng Pfs25, antibody levels did not decrease to half of the day 42 levels by day 250, corresponding to an antibody half-life of greater than 250 days (Fig 4a). Antigen-specific, long-lived plasma cells ($CD138^+$, $B220^-$) were detected in the bone

marrow of mice on day 250 (Fig 4b and Fig S15), confirming an immunological basis for the long-lived antibody response. Serum drawn from mice at day 250 was active in transmission blocking based on the SMFA (Fig 4c).

Additional adjuvants were compared with CoPoP/PHAD in a head-to-head study. Commercial adjuvants included Alum, TiterMax, AdjuPhos, QuilA, Sigma Adjuvant System, Addavax (similar to MF59) and Freund's adjuvant (CFA/IFA). A 100 nm formulation containing dioleoylphosphatidylcholine, PHAD and QS21 was prepared with similar composition as AS01.[41] Only the CoPoP/PHAD adjuvant induced high levels of Pfs25 antibodies with 100 ng Pfs25, presumably owing to the important of antigen particleization (Fig 5a). Despite the potent response, CoPoP/PHAD liposomes with Pfs25 produced the least amount of local reactogenicity of all the adjuvants assessed when injected intradermally in the footpad, as assessed by swelling (Fig 5b).

The effect of Pfs25 density on the liposomes was assessed with a 10 ng low-dose of Pfs25. Density was compared under standard conditions (estimated at 121 proteins per liposome based on protein binding, liposome diameter, and geometrical considerations[42]), and a reduced density of just 5 % of that amount (6 proteins per liposome). The higher density antigen resulted in more production of anti-Pfs25 IgG by approximately an order of magnitude (Fig S16a). However, post-immune sera for both high and low antigen density fully inhibited parasite development in the SMFA (Fig S16b), implying that a sufficient level of antibodies was induced to saturate the assay. We conclude that the SNAP approach is effective at generating functional antibodies over a wide range of antigen densities, even at low antigen injected doses.

The use of CoPoP/PHAD liposomes that are combined with separately-produced antigen at the time of immunization may have advantages in modular research and early phase clinical trials, since only a single batch of sterile liposomes would be required. However, it could eventually be beneficial to develop a single vial formulation without the requirement of a mixing step. We assessed whether Pfs25, once bound to CoPoP/PHAD liposomes, would be a stable formulation. As shown in Fig S17a-c, Pfs25 binding remained intact over a month-long period, as did liposome size and polydispersity. No free protein was detected by native PAGE following a month and a half of storage (Fig S17d). When electrophoresis was performed under reducing and denaturing conditions (which triggers release of the his-tagged protein), no Pfs25 degradation was observed (Fig S17e). Pfs25 that was pre-incubated for multiple weeks at 4 °C prior to vaccination (100 ng for both prime and boost) induced no difference in IgG generation (Figure S17f). Thus, the SNAP approach could be applicable to both bedside mixing, or for generating batches of particleized liposomes.

Antigen multiplexing

The multistage life cycle of *Plasmodium* species, in which different proteins are exposed on the parasite surface at different stages, may be a contributing factor to the difficulty of creating an effective malaria vaccine. Multistage, multi-antigen malaria vaccines are considered to be a promising avenue of research.[43] However, the process of developing and biochemically characterizing multistage, multi-antigen vaccines is challenging. CoPoP/

PHAD liposomes could facilitate this process since well-defined his-tagged antigens can easily be mixed with the liposomes to undergo SNAP. The antigen composition would be easily adjustable and no chemical conjugation or purification steps are required.

We examined a panel of his-tagged *P. falciparum* antigens expressed at different stages the parasite life-cycle. The concept is that these antigens could all be combined into a single particle by simple mixing prior to immunization (Fig 6a). AMA-1 is a blood stage antigen candidate expressed inside schizonts.[44] Pfg27 is produced in gametocytes.[45] Pfs230 is an antigen candidate expressed in sexual-stage gametocytes and gametes. The NANP peptide is a repeating sequence found in the circumsporozoite protein (CSP), a pre-erythrocytic stage antigen expressed on sporozoites.

The binding of each his-tagged protein antigen (Pfg27, Pfs25, Pfs230, AMA-1), and the multiplexed combination, was assessed using native PAGE (Fig 6b). When incubated with CoPoP/PHAD liposomes, the proteins bound efficaciously and no free protein bands were seen on the gel. The proteins had appropriate size and charge to enable the multiplexed antigen binding to also be confirmed with individually resolved antigens. Microcentrifugal filtration confirmed the binding of each antigen to CoPoP/PHAD liposomes, but not identical liposomes lacking cobalt (Fig 6c). Following antigen binding, the size of the multiplexed liposomes remained around 100 nm (Fig 6d), and the polydispersity was less than 0.3 (Fig S18). Thus, CoPoP liposomes are amenable for SNAP of multiple antigens, simultaneously.

Mice were immunized with 100 ng of each antigen, either individually or multiplexed. A fixed mass ratio of [PHAD: antigens] of [4:1] was used in all cases. When immunized with individual antigens, specific IgG was induced for all antigens without cross-reactivity (Fig 2e). The multiplexed SNAP vaccine resulted in high IgG production against all the antigens. Alum was ineffective for multiplexing antigens, with significant IgG levels only detected for one (out of five) antigens; Pfs230. Analysis of the SNAP multiplexed response revealed a slight decrease in the IgG levels against Pfs25 and Pfs230, compared to their single antigen vaccination counterparts. Conversely, there was a substantial increase in the anti-CSP IgG titer of the multiplexed vaccine. A duplex vaccine of Pfs25 combined with NANP was sufficient to generate increased levels of anti-CSP IgG (Fig S19).

Next, we investigated whether multiplexed SNAP immunization induced antibodies that recognize native *P. falciparum* proteins. Different life stages of the parasite, including sporozoites, ookinetes, gametocytes, schizonts were subjected to an immunofluorescence assay (IFA). Post-immune sera from mice immunized with individual his-tagged antigens exhibited expected patterns of reactivity with the individual life stages of parasites (Fig 6f, Fig S20). The post-immune sera from mice SNAP immunized with multivalent antigens recognized all expected life-stages of the parasite. Multiplexed antigens adjuvanted with Alum did not induce effective antibodies, with the only response being observed with Pfs230. The mechanism by which SNAP immunization exerts a balanced immune response requires further characterization, but may relate to the low antigen dose used or improved and balanced antigen uptake in APCs.

Conclusion

Recombinant his-tagged proteins spontaneously bind to liposomes containing CoPoP. This enables the rapid, gentle and uniformly-oriented particleization of well-characterized, purified his-tagged antigens. The SNAP approach safely induced durable antibody responses orders of magnitude greater than other adjuvants. Functional antibodies were induced with nanograms of Pfs25, showing potential for antigen-sparing practices. SNAP immunization was well-suited for multiplexed immunization with at least 5 his-tagged antigens, an approach that may be of interest for developing recombinant vaccines that target different life-stages of the malaria parasite.

Methods

See Supporting Methods section for additional details.

Materials:

His-tagged Pfs25 was produced in a baculovirus system as previously described.[10] His-tagged plant-derived Pfs25 for ELISA coating was produced in *Nicotiana benthamiana* as previously reported.[46] His-tagged Pfs230 was produced in a baculovirus system as previously reported.[47] His-tagged Apical Membrane Antigen-1 (AMA1) was produced in *E. coli* as previously reported.[48] His-tagged Pgf27 (MRA-1274) was obtained from BEI Resources, and a $(NANP)_6$-$(His)_7$ peptide was synthesized by GenScript. CSP for ELISA was produced in *E. coli* as previously reported.[49] CoPoP was produced as previously described.[23] The following adjuvants were obtained: Addavax (InvivoGen Cat. # vac-adx-10), Adju-Phos (InvivoGen Cat. # vac-phos-250), Quil-A® (InvivoGen Cat. # vac-quil), TiterMax® Gold Adjuvant (Sigma Cat. # T-2684), Sigma Adjuvant System (Sigma Cat. # S-6322), Imject™ Incomplete Freund's Adjuvant for prime and Freund's Complete Adjuvant for boost (IFA and CFA, Fisher Cat. # 77145 and 77140), Montanide ISA720 (SEPPIC) and Alhydrogel 2% aluminum gel (Accurate Chemical And Scientific Corporation; Cat. # A1090BS). The following lipids were used: 1,2-dipalmitoyl-sn-glycero-3-phosphocholine (DPPC, Corde Cat. # LP-R4–057), Ni-NTA lipid dioleoylglycero-Ni-NTA (Avanti Cat. # 790404P), 1,2-Dioleoyl-sn-glycero-3-phosphocholine (DOPC, Avanti #850375), cholesterol (PhytoChol, Wilshire Technologies), PEG-lipid (DSPE-PEG2K, Corden Cat. # LP-R4–039), synthetic monophosphoryl lipid A Phosphorylated HexaAcyl Disaccharide (PHAD, Avanti Cat. # 699800P) and (3-deacyl)-(6-acyl) PHAD (3D6A, Avanti Cat. # 699855P). QS21 obtained from Desert King. Granulocyte-macrophage colony-stimulating factor (GM-CSF) was obtained from Shenandoah Biotechnology (Cat. # 200–15-AF). Cytochalasin B was obtained from ThermoFisher Scientific (Cat. # 14930–96-2).

Cell studies:

RAW264.7 murine macrophage cells were obtained from ATCC and cultured in in Dulbecco's modified Eagle's medium (DMEM) with 10 % fetal bovine serum (FBS) and 1% penicillin/streptomycin.

BMDC were derived from bone marrow cells obtained from CD-1 mice. Bone marrow was collected from the femurs and tibia of mice. The concentration of cells was seeded at 10^7 cells/ml and cultured in 10 cm petri dish in RPMI 1640 culture medium with 10 % FBS and 20 ng recombinant GM-CSF on day 0. On day 3, an additional 10 mL medium containing GM-CSF was added into the petri dish so the final volume of the medium was 20 mL. On day 6, non-adherent cells were collected and cultured in a 24-well plate at 5×10^5 cell/mL in RPMI culture medium containing 10% FBS and 1% Pen/Strep, and then incubated for 24 hr with CoPoP/PHAD, CoPoP, and PBS mixed at 1 μg/mL Pfs25, with a fixed 4:1 mass ratio of CoPoP to Pfs25. Cells were washed with PBS containing 0.1% BSA for 3 times, and stained with antibodies against CD11c, CD40, CD80 and MHC-II for 1 hr on ice prior to flow cytometry.

For *in vitro* uptake studies, RAW264.7 and BMDC (5×10^5/well) were cultured in 24-well plate overnight to reach 70–80% confluence. Cells were then treated with (i) various types of liposomes with 1 μg/mL of Pfs25–488 or (ii) pre-incubated with Cytochalasin B (10 μg/mL) for 1 hr before the uptake study. For quantification, after incubation for 4 hr, the cells were harvested, washed with PBS 3 times and treated with lysis buffer (1% Triton X-100 and 0.1% SDS in PBS). The fluorescence signal was measured and the cellular Pfs25 uptake was calculated by first preparing a Pfs25–488 standard curve and calculating the concentration based on the standard curve.

Liposome preparation:

Liposomes were prepared by ethanol injection and nitrogen-pressurized lipid extrusion in phosphate buffered saline (PBS) carried out at 60 °C followed by dialysis to remove ethanol. For liposomes containing QS21, QS21 (1 mg/mL) was added to the liposomes after formation at an equal mass ratio as PHAD. Final liposome concentration was adjusted to 320 μg/mL PHAD and were passed through a 0.2 um sterile filter and stored at 4 ° C. Liposome sizes and polydispersity index were determined by dynamic light scattering with a NanoBrook 90 plus PALS instrument after 200-fold dilution in PBS. The standard CoPoP/PHAD liposome formulation had a mass ratio of [DPPC:CHOL:PHAD:CoPOP] [4:2:1:1] and other formulations are detailed in the supporting information.

SNAP characterization:

Protein binding with Pfs25 or lysozyme (VWR Cat. # 97062–138) was carried out by incubating protein and liposomes with a 1:4 mass ratio of protein:PHAD, unless stated otherwise. Following incubation, the sample was subjected to microcentrifugal filtration (PALL Cat. # 29300) and protein in filtrate was assessed by micro BCA (Thermo Cat. # 23235). For gel electrophoresis, loading dye was added to liposome samples and loaded into PAGE gels (Lonza Cat. # 8522) and subjected to electrophoresis and staining. Cryogenic transmission electron microscopy was carried out as described in the supporting information. Samples for immunization were prepared in the same way, but diluted in PBS to achieve the desired antigen dosing, with the antigen:PHAD mass ratio remaining constant (1:4).

SNAP multiplexing:

Multiplexing was carried out by mixing CoPoP/PHAD liposomes with 5 different his-tagged malaria antigens (Pfs25, Pfs230, Pfg27, AMA-1 and NANP), for 3 hr at RT in the same way as Pfs25. A constant mass ratio of antigen:PHAD of 1:4 was maintained in all cases.

Murine immunization and serum analysis:

8-week-old female CD-1 mice received intramuscular (IM) injections on days 0 and 21 containing indicated antigen doses combined with indicated adjuvants. Serum was collected on day 42 unless otherwise indicated and sent to the Laboratory of Malaria and Vector Research at the National Institute of Allergy and Infectious Diseases (NIAID) for anti-Pfs25 ELISA[50] and SMFA[51, 52] analysis which was carried out as previously described. Supporting Tables S1-S5 report the raw SMFA data.

Rabbit immunization:

10–12 weeks old female New Zealand white rabbits received intramuscular injections on days 0 and 28 of 1 μg or 10 μg Pfs25 adjuvanted with CoPoP/PHAD (4 or 40 μg PHAD) liposomes or 10 μg Pfs25 with Alum. Serum were collected on day 0, 28 and day 56. Serum was sent to NIAID for ELISA and SMFA analysis.

Flow cytometry:

Flow cytometry studies were carried out using a BD LSRFortessa™ X-20 cytometer. Flowjo (version 10) software was used for data analysis.

For draining lymph node studies of Pfs25 uptake in immune cells, mice were intramuscularly immunized with 1 μg of Pfs25-oyster488 conjugate. 2 days after injection, mice were sacrificed and inguinal lymph nodes were collected. Cells were extracted and fixed with 4% paraformaldehyde at room temperature for 15 min, washed three times with 3 mL PBS by centrifugation at 500 rcf for 5 min. 5×10^5 cells per tube were stained for 30 min at room temperature with the following murine antibodies against I-A/I-E, B220, CD11c or F4/80 (all from BioLegend).

For staining marrow cells, on day 250, mice were sacrificed and bone marrow was collected. Marrow cells were counted, fixed with 4% paraformaldehyde at room temperature for 15 min in the dark, washed thrice with PBS and frozen in 10% DMSO. Cells were stained with anti-CD138 and anti-B220 antibodies (Biolegend) for 30 min at room temperature in dark, and followed by 3 PBS washes. Cells were permeabilized with 0.1 % Triton X-100 and stained with Pfs25-oyster488, followed by additional washing prior to flow cytometry.

For GC cells and Tfh cell populations, mice received 100 ng Pfs25 adjuvanted with CoPoP/PHAD or Alum. 14 days after immunization, mice were sacrificed and the inguinal LN were collected. Cells extracted from the lymph nodes were fixed with 4% paraformaldehyde for 15 min at room temperature, washed three times with 3 mL PBS with centrifugation at 500 rcf for 5 min. 5×10^5 cells per tube were than stained for 1 hr on ice with antibodies against B220, CD95, GL7. CD4, CXCR5 or PD-1 prior to flow cytometry.

For lymph node cell recruitment, mice were injected intramuscularly with CoPoP/PHAD liposomes or Alum with 100 ng of Pfs25. 48 hr after injection, mice were sacrifice and lymph nodes were collected for cell extraction. Cells were fixed with 4 % PDA for 15 min at room temperature, and washed with PBS for 3 times. Cells were stained with combination antibodies against Ly6C, CD11b, Ly6G, CD11c, CD3, I-A/I-E and F4/80, for 1 hr on ice. Cells were first gated with CD11c and CD11b (Fig S8A). Then, immune cells were identified based on surface marker in $CD11c^{high}$ and $CD11b^{low}$, neutrophils ($Ly6G^{high}$)(Fig S8D), eosinophils ($Ly6G^{int}$, $F4/80^{int}$, SSC)(Fig S8E), monocytes (Ly6C ^{high})(Fig S8C) and macrophage (F4/80 ^{high})(Fig S8B). Three types of DC cells were gated (Fig S8F), for myeloid DC, we first gated $Cd11c^{high}$ and $CD11b^{high}$, then gated MHC-II positive cells.

Acute toxicity studies:

8-week-old female CD-1 mice were treated with intramuscular injection of CoPoP/PHAD/Pfs25 prepared in the usual way with 20 μg Pfs25, or with intravenous injection of CoPoP/PEG liposomes (95:5 molar ratio of CoPoP:PEG) at 100 mg/kg CoPoP. Two weeks later, blood and serum were collected and subjected to standard complete blood cell count and serum panel (IDEXX Cat. # 98–20590-00). The organs, including kidney, lung, liver, spleen were fixed in formalin for 24 hr, and transfered to 70% EtOH and subjected to hematoxylin and eosin staining. Briefly, slides were dewaxed through xylenes and graded alcohols, transfered to water for 3 min, hematoxylin for 3 min, water for 3 min, 1% acid alcohol for 1 min, water for 3 min, 0.2% ammonium hydroxide for 3 min, water for 4 min, 95% ethanol for 3 min, Eosin for 30 seconds, then dehydrated through graded alcohols, cleared, mounted and coversliped with xylene mount prior to imaging.

Indirect immunofluorescence assay (IFA):

P. falciparum schizonts, gametocytes, ookinetes and sporozoites were obtained and fixed on slides as described in the supplementary methods. Slides were blocked with 5% BSA in PBS containing 0.1% Tween-20 for 30 min at 37 °C. Sera collected from mice immunized with individual or multiplexed antigens with SNAP or Alum was diluted 1:100 and incubated in 5% BSA in PBS with the fixed slides at 37 °C for 1 hr, followed by 3 times washing with PBS in a humidity chamber, each time for 5 min. FITC-conjugated goat anti-mouse IgG (1:1000) was then incubated with the slides for 30 min at 37 °C, followed by 3 times washing with PBS, each time for 5 min. The slides were mounted with Prolong gold antifade with DAPI (Thermo Fisher Cat. # P36931) and imaged with an EVOS FL microscope using a 100× objective lens.

Supplementary Material

Refer to Web version on PubMed Central for supplementary material.

Acknowledgements

This study was supported by PATH's Malaria Vaccine Initiative, grants from National Institutes of Health (R21AI122964 and DP5OD017898), and the intramural program of the National Institute of Allergy and Infectious Diseases/NIH. The authors acknowledge assistance from Godfree Mlambo and Abhai Tripathi with immunofluorescence assays, and valuable input from Carl Alving and Ashley Birkett.

References

1. WHO World Malaria Report 2017 (World Health Organization, Geneva; 2017).
2. Nunes JK et al. Development of a transmission-blocking malaria vaccine: Progress, challenges, and the path forward. Vaccine 32, 5531–5539 (2014). [PubMed: 25077422]
3. Birkett AJ Status of vaccine research and development of vaccines for malaria. Vaccine 34, 2915–2920 (2016). [PubMed: 26993333]
4. Barr PJ et al. Recombinant Pfs25 protein of Plasmodium falciparum elicits malaria transmission-blocking immunity in experimental animals. J Exp. Med 174, 1203–1208 (1991). [PubMed: 1940798]
5. Kaslow DC et al. A vaccine candidate from the sexual stage of human malaria that contains EGF-like domains. Nature 333, 74–76 (1988). [PubMed: 3283563]
6. Kaslow DC et al. Saccharomyces cerevisiae recombinant Pfs25 adsorbed to alum elicits antibodies that block transmission of Plasmodium falciparum. Infect. Immun 62, 5576–5580 (1994). [PubMed: 7960139]
7. Kumar R, Angov E & Kumar N Potent Malaria Transmission-Blocking Antibody Responses Elicited by Plasmodium falciparum Pfs25 Expressed in Escherichia coli after Successful Protein Refolding. Infect. Immun 82, 1453–1459 (2014). [PubMed: 24421036]
8. Gregory JA et al. Algae-Produced Pfs25 Elicits Antibodies That Inhibit Malaria Transmission. PLoS One 7, e37179 (2012). [PubMed: 22615931]
9. Mlambo G, Kumar N & Yoshida S Functional immunogenicity of baculovirus expressing Pfs25, a human malaria transmission-blocking vaccine candidate antigen. Vaccine 28, 7025–7029 (2010). [PubMed: 20709008]
10. Lee S-M et al. Assessment of Pfs25 expressed from multiple soluble expression platforms for use as transmission-blocking vaccine candidates. Malar. J 15, 405 (2016). [PubMed: 27515826]
11. Wu Y et al. Phase 1 Trial of Malaria Transmission Blocking Vaccine Candidates Pfs25 and Pvs25 Formulated with Montanide ISA 51. PLoS One 3, e2636 (2008). [PubMed: 18612426]
12. Malkin EM et al. Phase 1 vaccine trial of Pvs25H: a transmission blocking vaccine for Plasmodium vivax malaria. Vaccine 23, 3131–3138 (2005). [PubMed: 15837212]
13. Radtke AJ et al. Adjuvant and carrier protein-dependent T-cell priming promotes a robust antibody response against the Plasmodium falciparum Pfs25 vaccine candidate. Sci. Rep 7, 40312 (2017). [PubMed: 28091576]
14. Shimp RL, Jr. et al. Development of a Pfs25-EPA malaria transmission blocking vaccine as a chemically conjugated nanoparticle. Vaccine 31, 2954–2962 (2013). [PubMed: 23623858]
15. Miyata T et al. Plasmodium vivax Ookinete Surface Protein Pvs25 Linked to Cholera Toxin B Subunit Induces Potent Transmission-Blocking Immunity by Intranasal as Well as Subcutaneous Immunization. Infect. Immun 78, 3773–3782 (2010). [PubMed: 20584978]
16. Gregory JA, Topol AB, Doerner DZ & Mayfield S Alga-Produced Cholera Toxin-Pfs25 Fusion Proteins as Oral Vaccines. Appl. Environ. Microbiol 79, 3917–3925 (2013). [PubMed: 23603678]
17. Kumar R et al. Nanovaccines for malaria using Plasmodium falciparum antigen Pfs25 attached gold nanoparticles. Vaccine 33, 5064–5071 (2015). [PubMed: 26299750]
18. Kumar R et al. Potent Functional Immunogenicity of Plasmodium falciparum Transmission-Blocking Antigen (Pfs25) Delivered with Nanoemulsion and Porous Polymeric Nanoparticles. Pharm. Res 32, 3827–3836 (2015). [PubMed: 26113235]
19. Jones RM et al. A Plant-Produced Pfs25 VLP Malaria Vaccine Candidate Induces Persistent Transmission Blocking Antibodies against Plasmodium falciparum in Immunized Mice. PLoS One 8, e79538 (2013). [PubMed: 24260245]
20. Goodman AL et al. A viral vectored prime-boost immunization regime targeting the malaria Pfs25 antigen induces transmission-blocking activity. PLoS One 6, e29428 (2011). [PubMed: 22216279]
21. Li Y et al. Enhancing immunogenicity and transmission-blocking activity of malaria vaccines by fusing Pfs25 to IMX313 multimerization technology. Sci. Rep 6, 18848 (2016). [PubMed: 26743316]

22. Brune KD et al. Plug-and-Display: decoration of Virus-Like Particles via isopeptide bonds for modular immunization. Sci. Rep 6, 19234 (2016). [PubMed: 26781591]
23. Shao S et al. Functionalization of cobalt porphyrin-phospholipid bilayers with his-tagged ligands and antigens. Nat. Chem 7, 438–446 (2015). [PubMed: 25901823]
24. Lee S-M, Plieskatt J & King CR Disulfide bond mapping of Pfs25, a recombinant malaria transmission blocking vaccine candidate. Anal. Biochem 542, 20–23 (2018). [PubMed: 29162427]
25. Rüger R, Müller D, Fahr A & Kontermann RE In vitro characterization of binding and stability of single-chain Fv Ni-NTA-liposomes. J. Drug Targeting 14, 576–582 (2006).
26. Platt V et al. Influence of Multivalent Nitrilotriacetic Acid Lipid−Ligand Affinity on the Circulation Half-Life in Mice of a Liposome-Attached His6-Protein. Bioconj. Chem 21, 892–902 (2010).
27. Shao S et al. Functionalization of cobalt porphyrin–phospholipid bilayers with his-tagged ligands and antigens. Nat. Chem 7, 438–446 (2015). [PubMed: 25901823]
28. Bale S et al. Covalent Linkage of HIV-1 Trimers to Synthetic Liposomes Elicits Improved B Cell and Antibody Responses. J. Virol 91 (2017).
29. Scally SW et al. Molecular definition of multiple sites of antibody inhibition of malaria transmission-blocking vaccine antigen Pfs25. Nat. Commun 8, 1568 (2017). [PubMed: 29146922]
30. Beck Z et al. Differential immune responses to HIV-1 envelope protein induced by liposomal adjuvant formulations containing monophosphoryl lipid A with or without QS21. Vaccine 33, 5578–5587 (2015). [PubMed: 26372857]
31. Sauer SW & Keim ME Hydroxocobalamin: Improved public health readiness for cyanide disasters. Ann. Emergency Med 37, 635–641 (2001).
32. Kuzminski AM, Del Giacco EJ, Allen RH, Stabler SP & Lindenbaum J Effective Treatment of Cobalamin Deficiency With Oral Cobalamin. Blood 92, 1191–1198 (1998). [PubMed: 9694707]
33. Calabro S et al. Vaccine adjuvants alum and MF59 induce rapid recruitment of neutrophils and monocytes that participate in antigen transport to draining lymph nodes. Vaccine 29, 1812–1823 (2011). [PubMed: 21215831]
34. Liang F et al. Vaccine priming is restricted to draining lymph nodes and controlled by adjuvant-mediated antigen uptake. Sci. Transl. Med 9 (2017).
35. Manh TP, Alexandre Y, Baranek T, Crozat K & Dalod M Plasmacytoid, conventional, and monocyte-derived dendritic cells undergo a profound and convergent genetic reprogramming during their maturation. Eur. J. Immunol 43, 1706–1715 (2013). [PubMed: 23553052]
36. Ginhoux F et al. The origin and development of nonlymphoid tissue CD103+ DCs. J. Exp. Med 206, 3115–3130 (2009). [PubMed: 20008528]
37. Edelson BT et al. Peripheral CD103+ dendritic cells form a unified subset developmentally related to CD8alpha+ conventional dendritic cells. J. Exp. Med 207, 823–836 (2010). [PubMed: 20351058]
38. Rooijen NV & Sanders A Liposome mediated depletion of macrophages: mechanism of action, preparation of liposomes and applications. J. Immunol. Methods 174, 83–93 (1994). [PubMed: 8083541]
39. Allen TM, Austin GA, Chonn A, Lin L & Lee KC Uptake of liposomes by cultured mouse bone marrow macrophages: influence of liposome composition and size. Biochim. Biophys. Acta 1061, 56–64 (1991). [PubMed: 1995057]
40. Fan YC, Sahdev P, Ochyl LJ, Akerberg JJ & Moon JJ Cationic liposome-hyaluronic acid hybrid nanoparticles for intranasal vaccination with subunit antigens. J. Controlled Release 208, 121–129 (2015).
41. Cunningham AL et al. Efficacy of the Herpes Zoster Subunit Vaccine in Adults 70 Years of Age or Older. New Engl. J. Med 375, 1019–1032 (2016). [PubMed: 27626517]
42. Viswanathan S, Rani C, Vijay Anand A & Ho J.-a.A. Disposable electrochemical immunosensor for carcinoembryonic antigen using ferrocene liposomes and MWCNT screen-printed electrode. Biosensors Bioelectron 24, 1984–1989 (2009).
43. Doolan DL & Hoffman SL DNA-based vaccines against malaria: status and promise of the Multi-Stage Malaria DNA Vaccine Operation. Int. J. Parasitol 31, 753–762 (2001). [PubMed: 11403765]

44. Peterson MG et al. Integral membrane protein located in the apical complex of Plasmodium falciparum. Mol. Cell. Biol 9, 3151–3154 (1989). [PubMed: 2701947]
45. Lobo CA, Konings RN & Kumar N Expression of early gametocyte-stage antigens Pfg27 and Pfs16 in synchronized gametocytes and non-gametocyte producing clones of Plasmodium falciparum. Mol. Biochem. Parasitol 68, 151–154 (1994). [PubMed: 7891740]
46. Farrance CE et al. Antibodies to plant-produced Plasmodium falciparum sexual stage protein Pfs25 exhibit transmission blocking activity. Hum Vaccin 7 Suppl, 191–198 (2011).
47. Lee SM et al. An N-terminal Pfs230 domain produced in baculovirus as a biological active transmission-blocking vaccine candidate. Clin. Vaccine Immunol (2017).
48. Dutta S et al. High antibody titer against apical membrane antigen-1 is required to protect against malaria in the Aotus model. PLoS One 4, e8138 (2009). [PubMed: 19997632]
49. Genito CJ et al. Liposomes containing monophosphoryl lipid A and QS-21 serve as an effective adjuvant for soluble circumsporozoite protein malaria vaccine FMP013. Vaccine 35, 3865–3874 (2017). [PubMed: 28596090]
50. Miura K et al. Development and Characterization of a Standardized ELISA Including a Reference Serum on Each Plate to Detect Antibodies Induced by Experimental Malaria Vaccines. Vaccine 26, 193–200 (2008). [PubMed: 18054414]
51. Quakyi IA et al. The 230-Kda Gamete Surface Protein of Plasmodium-Falciparum Is Also a Target for Transmission-Blocking Antibodies. J. Immunol 139, 4213–4217 (1987). [PubMed: 2447164]
52. Cheru L et al. The IC(50) of anti-Pfs25 antibody in membrane-feeding assay varies among species. Vaccine 28, 4423–4429 (2010). [PubMed: 20434549]

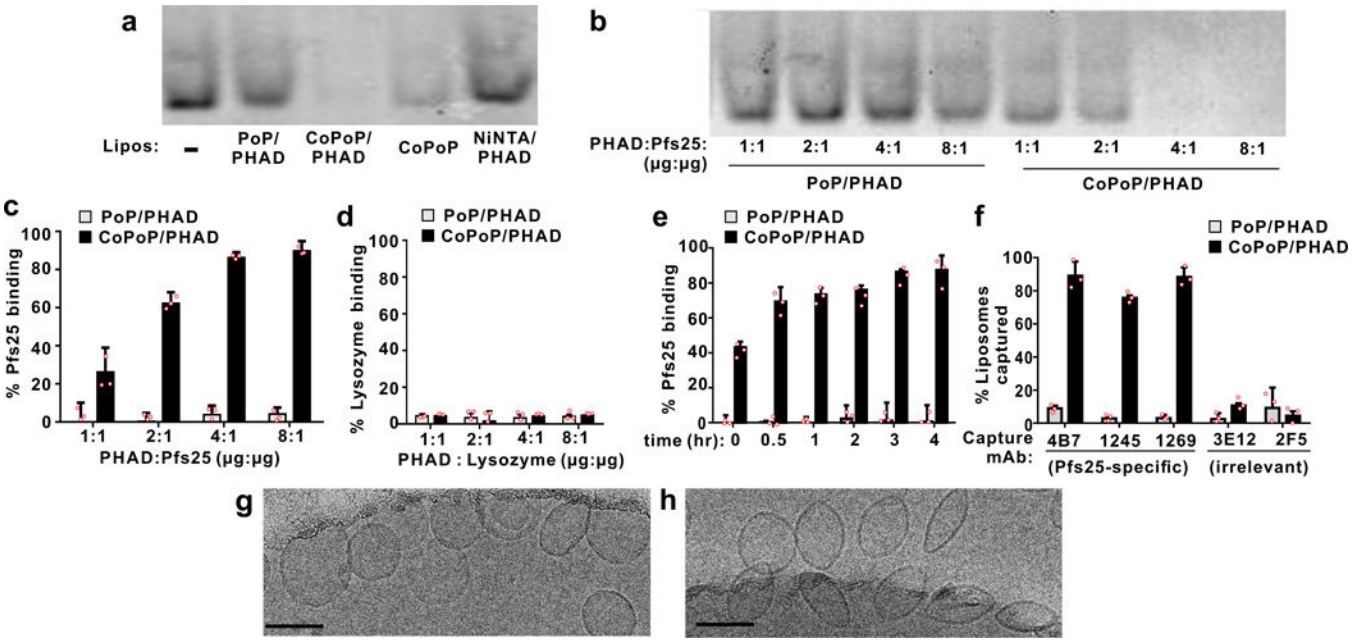

Fig 1. Spontaneous nanoliposome antigen particle-formation (SNAP) with his-tagged Pfs25.

a, Native PAGE of his-tagged Pfs25 after 3 hr incubation with the indicated liposomes at a 4:1 PHAD:protein (or analogous) ratio. **b,** Native PAGE of 1 μg Pfs25 incubated with varying liposome amounts. **c,** Protein binding determined by microcentrifugal filtration using Pfs25 (**c**) or non-his-tagged lysozyme (**d**). e**,** Kinetics of Pfs25 binding to PoP or CoPoP liposomes at room temperature. **f,** Immunoprecipitation of Pfs25-bound liposomes by Pfs25-specific monoclonal antibodies. Cryo-electron micrographs of CoPoP/PHAD liposomes with (**g**) or without (**h**) incubation with Pfs25 for 3 hrs. A 100 nm scale bar is shown. Images are from a single experiment. Data in **a** and **b** are representative of 3 independent experiments. Bar graphs show mean +/−std. dev. for n=3 independent experiments.

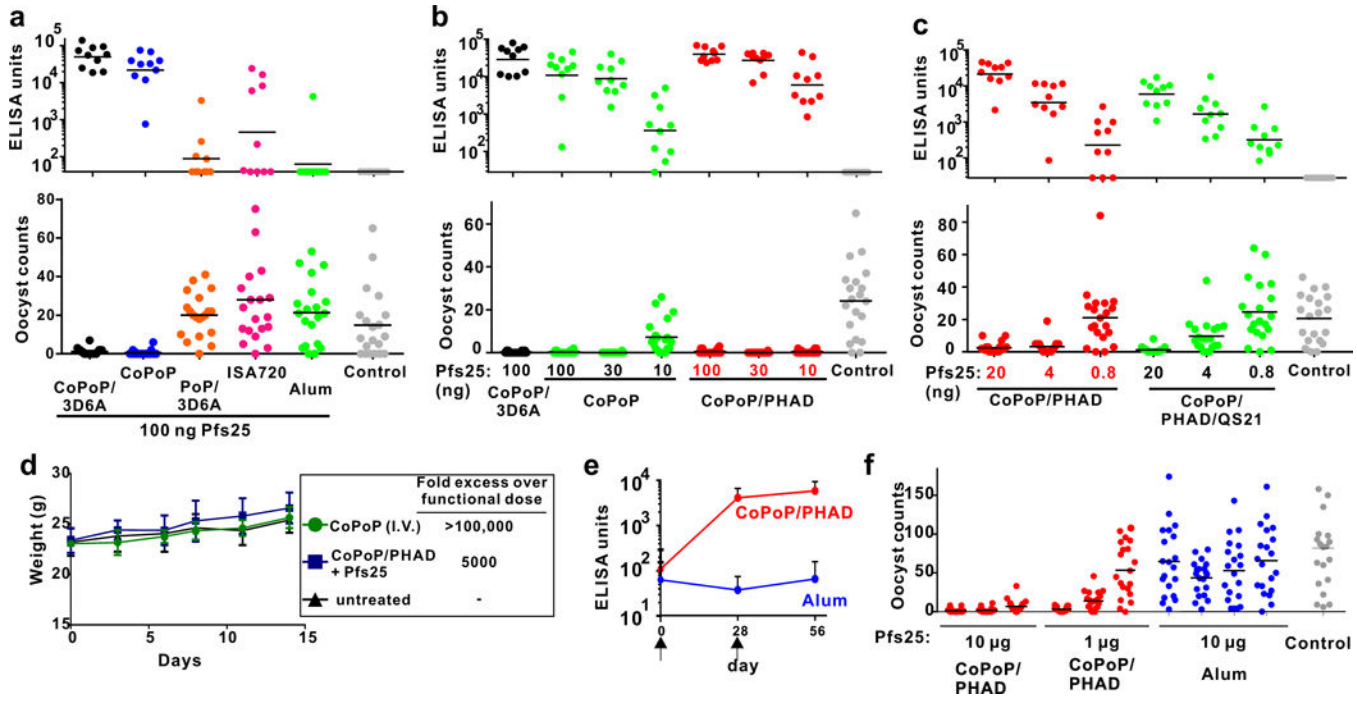

Fig 2. Pfs25 SNAP immunization in mice (a-d) and rabbits (e,f).

a, b, c: Anti-Pfs25 IgG ELISA data (top) and standard membrane feeding assay functional assay (SMFA, bottom). Mice were intramuscularly immunized on day 0 and day 21 with indicated Pfs25 doses, and serum was collected on day 42 and assessed. **a,** Immunization with 100 ng Pfs25, mixed with indicated adjuvants just prior to injection. **b,** Dose de-escalation of Pfs25 with CoPoP or CoPoP/PHAD liposomes; **c,** Dose de-escalation of Pfs25 with CoPoP/PHAD liposomes with or without QS21. Control groups correspond to various CoPoP adjuvants without Pfs25. **d,** Mouse weight following extreme CoPoP dosing. CoPoP alone liposomes were intravenously (I.V.) injected at a CoPoP dose of 100 mg/kg. Another group of mice was given a single vaccination with 20 µg Pfs25 adjuvanted with CoPoP/PHAD at the standard 1:4 (µg:µg) Pfs25:PHAD ratio. Mean +/−std. dev. for n=5 mice. **e,** IgG ELISA titer in rabbits immunized with 10 µg Pfs25 at time points indicated by arrows. Geometric Mean is shown +/−std. dev. for n=3 (CoPoP/PHAD) or n=4 (Alum) rabbits. **f,** SMFA with the sera of individual rabbits immunized as indicated. ELISA experiment in **a-c** were performed with n=10 of independent mice and lines show geometric mean. SMFA experiments in **a-c** and **f** were performed with n=20 mosquitoes and lines show arithmetic mean. A fixed mass ratio of 4:1 Pfs25 to PHAD (or equivalent) was maintained in all experiments.

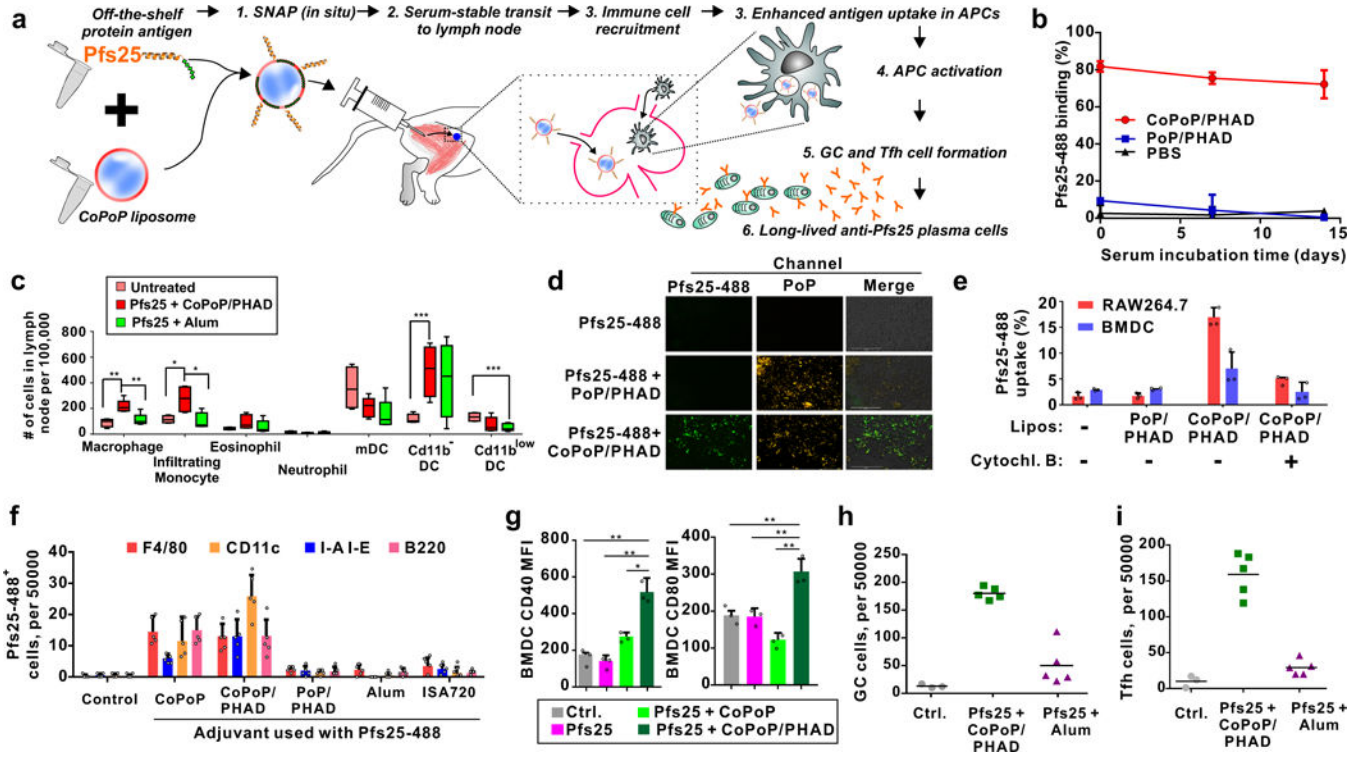

Figure 3: Mechanistic insights into SNAP immunization.

a, Putative steps in SNAP immunization. **b,** Particleization stability in 20% human serum at 37 °C. **c,** Immune cell populations in draining lymph nodes 48 hours after intramuscular Pfs25 immunization. Data show box-and-whiskers plot (n=5 mice per group). The line represents the median, the whiskers show data range and the box shows the interquartile range. **d,** Fluorescence microscopy of RAW264.7 macrophages after incubation with Pfs25 and liposomes. Bar: 100 μm. Representative images from 3 independent experiments. **e,** Pfs25 uptake following incubation with murine RAW264.7 or BMDC cells. Cytochalasin B was used as a phagocytosis inhibitor. **f,** Pfs25 uptake in immune cells in draining lymph nodes of mice, 48 hours after intramuscular administration. Lymph nodes cells were assessed for Pfs25–488 uptake with flow cytometry and co-staining with indicated surface markers. **g,** Activation of BMDCs as assessed by CD40 or CD80 mean fluorescence intensity (MFI) following incubation with 1 μg/mL of Pfs25 for 24 hr. (**h**) Germinal center (GC) cells ($GL7^+CD95^+$; within the $B220^+$ cell population) and **(i)** Tfh cells ($CXCR5^+PD\text{-}1^+$; within the $CD4^+$ cell population) in draining lymph nodes, 7 days after intramuscular immunization with 100 ng Pfs25. **b,** line shows mean +/−std. dev. for n=3 experiments. **f**, bars shows mean +/−std. dev. with n=5 mice per group. **e** and **g**, value shows mean +/−std. dev. for n=3 biologically independent experiments. **h** and **i,** lines show mean for n=5 mice per group. Asterisks show significance for unpaired, two-tailed Student's T – test: * $p<0.05$; ** $p<0.01$; *** $p<0.005$.

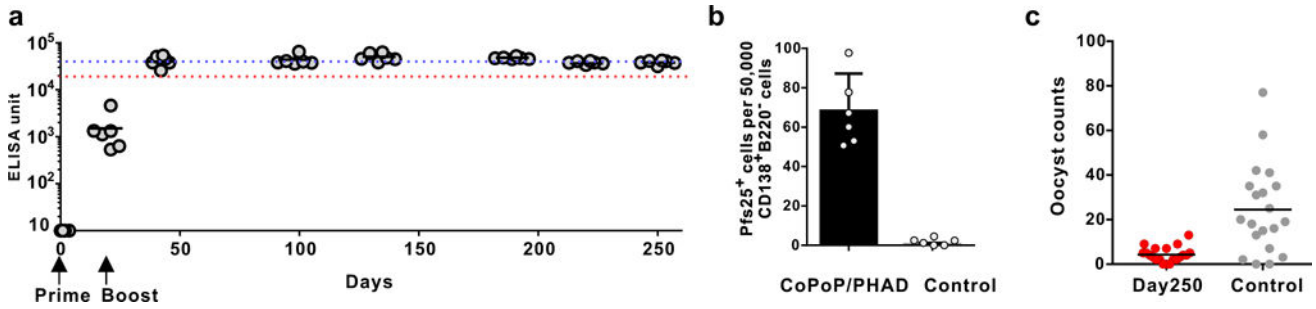

Fig 4. Durability of the anti-Pfs25 IgG response with SNAP immunization.

Mice were immunized intramuscularly with 100 ng Pfs25 mixed with CoPoP/PHAD liposomes (400 ng PHAD) on day 0 and 21, as indicated by the arrows. **a,** Serum was sampled periodically and assessed for anti-Pfs25 IgG. The blue and red lines show the 4×10^4 and 2×10^4 point on the y-axis, respectively, black lines show the geometric mean for n=6 mice. **b,** On day 250, bone marrow was assessed for antigen-specific, long-lived plasma cells by flow cytometry ($B220^-CD138^+$; staining positive for intracellular binding to fluorescent Pfs25). Bar graph shows mean +/−std. dev. for n=6 mice per group. **c,** Pooled mouse sera was collected from mice on day 250 and assessed with SMFA. Lines show mean for n=20 mosquitos per group.

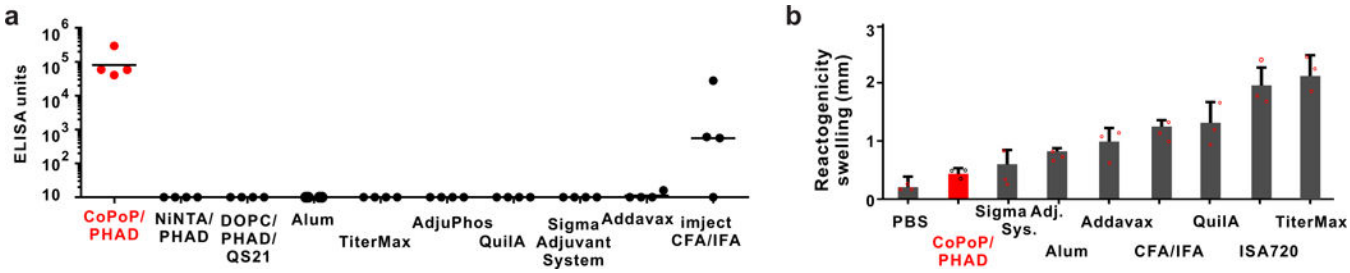

Fig 5. Immunization potency and local reactogenicity of SNAP compared to other adjuvants (all mixed prior to injection)

a, Comparison of anti-Pfs25 IgG titer for 100 ng Pfs25 vaccinated with indicated adjuvants, which were combined with Pfs25 prior to injection. Each ELISA point represents the anti-Pfs25 IgG titer of an individual mouse. Lines show geometric mean (n=4 mice per group). CD-1 mice were vaccinated intramuscularly with priming on day 0, boosting on day 21 and serum collection on day 42. **b,** Local reactogenicity of 100 ng Pfs25 injected in the footpad of CD-1 mice as measured by swelling, bar graph shows mean +/−std. dev. for n=3 mice per group.

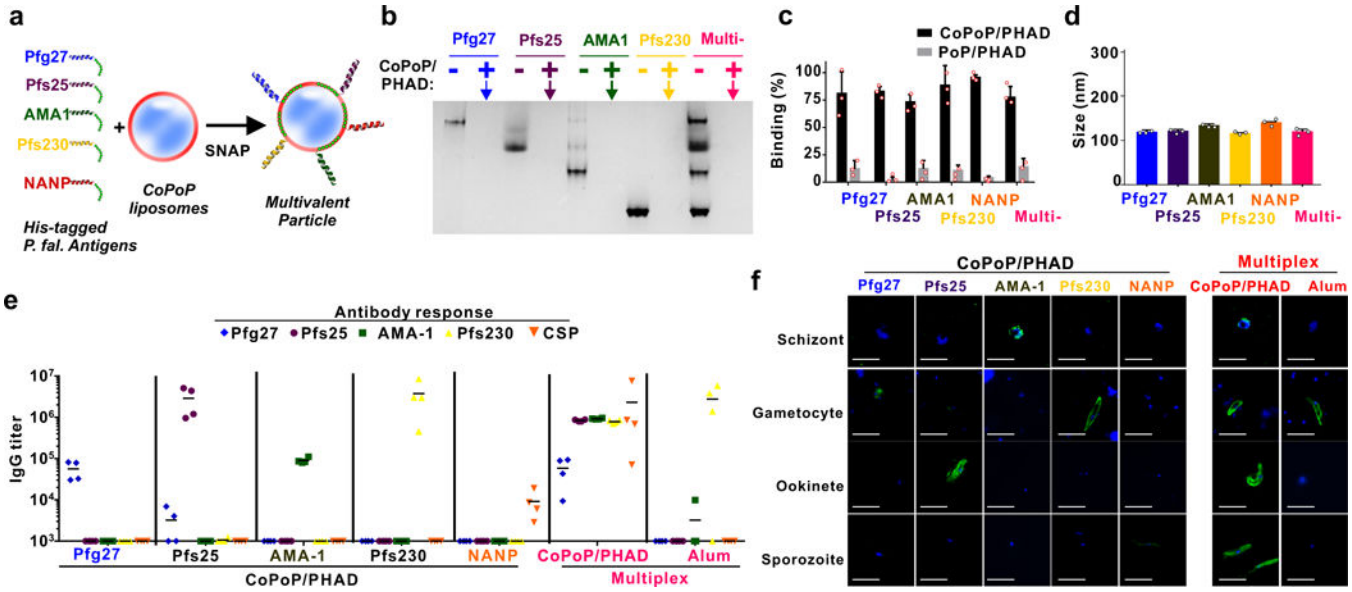

Fig 6. Multiplexed SNAP with *P. falciparum* antigens.

a, Schematic representation of multivalent SNAP. **b,** Native PAGE gel demonstrating effective single and multiplexed antigen binding to CoPoP/PHAD liposomes. The absence of a protein band indicated by the arrow reflects antigen binding to the liposomes, which are too large to enter the gel. **c,** Single and multiplexed antigen binding as assessed by microcentrifugal filtration. **d,** Size of liposomes following SNAP. **e,** ELISA against the indicated antigens in mice immunized with individual antigens or multiplexed combination of all antigens. Lines show geometric means for n=4 mice per group. **f,** Immunofluorescence assay of indicated post-immune sera with fixed parasites. Bar: 10 μm. For **c** and **d**, error bars show mean +/−std. dev. for n=3 independent experiments. **b** and **f** show representative results of 3 independent experiments.